

# Kinetics and Mechanism of the Outer-Sphere Oxidation of Horse-Heart Cytochrome *c* by an Anionic Chromium(v) Complex – Kinetic Evidence for Precursor Formation and a Late Electron-Transfer Transition State

Manuela Körner<sup>[a]</sup> and Rudi van Eldik<sup>\*[a]</sup>

**Keywords:** Cytochrome *c* / Chromium(v) / Saturation kinetics / Separation of *K* and *k*<sub>ET</sub> / Volume profile / Kinetics

The irreversible outer-sphere electron-transfer reaction between *trans*-bis(2-ethyl-2-hydroxybutanoato(2-))oxochromate(v) and cytochrome *c*<sup>II</sup> was investigated as a function of pH, concentration, temperature and pressure. The plot of the observed pseudo-first order rate constant as a function of the Cr<sup>V</sup> concentration shows a clear trend towards saturation at higher Cr<sup>V</sup> concentrations, from which the precursor formation constant and the electron-transfer rate constant could be separated (*K* = 37 ± 5 M<sup>-1</sup> and *k*<sub>ET</sub> = 1510 ± 180 s<sup>-1</sup> at pH 4.8 and 279 K). In the low Cr<sup>V</sup> concentration range the second-order electron-transfer rate constants were measured as a function of temperature ( $\Delta H^\ddagger = 20.9 \pm 0.6$  kJ mol<sup>-1</sup>;  $\Delta S^\ddagger = -79.9 \pm 2.1$  J K<sup>-1</sup> mol<sup>-1</sup>;  $\Delta G^\ddagger$  (279 K) = 43.2 kJ mol<sup>-1</sup>).

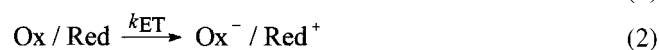
High-pressure experiments were performed at two different pH values. The kinetic (stopped-flow) and thermodynamic (electrochemical) measurements as a function of pressure enabled the construction of a volume profile for the system at 279 K. The activation volumes for the redox process are  $-9.2 \pm 0.2$  (pH 5.0) and  $-11.1 \pm 0.8$  cm<sup>3</sup> mol<sup>-1</sup> (pH 4.7), and the overall reaction volumes were estimated to be  $-7 \pm 2$  (pH 5.0) and  $-10 \pm 2$  cm<sup>3</sup> mol<sup>-1</sup> (pH 4.7). The transition state of the redox reaction lies to a large extent on the product side and can be described as "late". The results are discussed in comparison to earlier measurements using cobalt and ruthenium complexes as reaction partners for cytochrome *c*.

## Introduction

Cytochrome *c* typically undergoes outer-sphere electron-transfer reactions with metal complexes such as Co(phen)<sub>3</sub><sup>2+/3+</sup>, Co(terpy)<sub>2</sub><sup>2+/3+</sup>, or Ru(NH<sub>3</sub>)<sub>5</sub>py<sup>2+/3+</sup> (phen = 1,10-phenanthroline; terpy = 2,2':6',2''-terpyridine).<sup>[1–3]</sup> This type of mechanism includes the formation of an outer-sphere precursor complex as a result of electrostatic interactions (Equation 1), a subsequent rate-determining electron-transfer step *k*<sub>ET</sub> (Equation 2), and the dissociation of the successor complex to the final redox products (Equation 3).

Under pseudo-first-order conditions, i.e. at least a 10-fold excess of one of the reactants (viz. Red), and under the condition that the reaction proceeds to completion, this general mechanism leads to the rate law given by Equation 4.

For most systems *K*[Red] << 1, since the reactants are of similar charge, such that *K* is very small. Under these circumstances, the measured second-order rate constants



$$k_{\text{obs}} = \frac{K \cdot k_{\text{ET}} [\text{Red}]}{1 + K [\text{Red}]} \quad (4)$$

represent *K*·*k*<sub>ET</sub>. If *K*[Red] >> 1, then the observed rate constants become independent of the [Red] at high concentrations of Red and the limiting rate constant *k*<sub>ET</sub> is reached. In the case of highly negatively charged Fe(CN)<sub>6</sub><sup>4-/3-</sup> ions, saturation kinetics for the reaction with cytochrome were reported.<sup>[4]</sup> However, in later work it was demonstrated that the interpretation of the observed saturation kinetics was complicated by the fact that the reaction is reversible.<sup>[5]</sup> This led to a significant intercept in the plots of *k*<sub>obs</sub> versus concentration, such that the saturation in *k*<sub>obs</sub> at high concentrations could not be observed anymore.

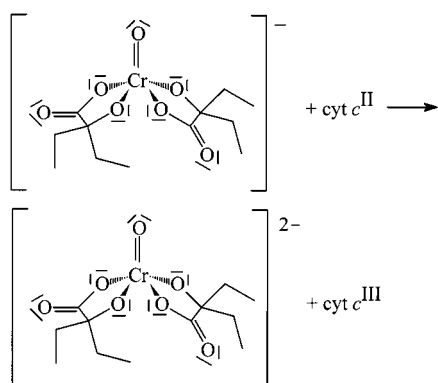
In principle, it should be possible to tune the extent of precursor formation by selecting reactants of high and opposite charge. This has been attempted in a number of cases,<sup>[5–7]</sup> but to our knowledge real rate saturation has only been found in studies of the reduction of cytochrome *c* by chromous ion and dithionite.<sup>[8][9]</sup> In all other cases, the observed second-order rate constant for the outer-sphere mechanism represents the product *K*·*k*<sub>ET</sub>, and values of *K* and *k*<sub>ET</sub> can only be separated by using a theoretical approach. With the aid of the Fuoss Equation,<sup>[10][11]</sup> a precursor formation constant of 3 M<sup>-1</sup> for the reaction of cytochrome *c* with positively charged metal complexes such as Ru(NH<sub>3</sub>)<sub>5</sub>py<sup>2+/3+</sup>, and a value of 200 M<sup>-1</sup> for the reaction with Fe(CN)<sub>6</sub><sup>4-/3-</sup> was calculated.

In our earlier work we have studied the outer-sphere electron-transfer reactions between cytochrome *c* and complexes of the type Ru(NH<sub>3</sub>)<sub>5</sub>X<sup>2+/3+</sup> (X = ammonia, pyridine, 4-ethyl-pyridine, isonicotinamide and 3,5-lutidine), as well as a series of chelated Co(II/III) diimine complexes.<sup>[12–14]</sup> In these systems precursor formation was so weak that *K* and *k*<sub>ET</sub> could not be separated kinetically.

<sup>[a]</sup> Institute for Inorganic Chemistry, University of Erlangen-Nürnberg, Egerlandstraße 1, D-91058 Erlangen, Germany  
Fax: (internat.) +49(0)9131/85–27387  
E-mail: vaneldik@chemie.uni-erlangen.de

However, the driving force of these reactions was so low that the kinetics of these redox reactions could be studied in both directions. This enabled us to construct volume profiles from high-pressure kinetic and thermodynamic data for the reversible electron-transfer processes, from which information on the location of the transition state in terms of volume changes along the reaction coordinate could be obtained. The volume profiles turned out to be highly symmetrical with the transition state located approximately halfway between the reactant and product states. The overall volume changes could be shown to be mainly due to intrinsic and solvational volume changes on the redox partner of cytochrome *c*, since cytochrome *c* itself undergoes almost no volume change during the electron-transfer process.<sup>[15]</sup>

In the present study we have selected an anionic Cr(V) complex, *trans*-bis(2-ethyl-2-hydroxybutanoato(2-))oxochromate(V), as the redox partner for cytochrome *c*. This complex has several negatively charged donor centers that could interact in a specific way with the positive charges on the surface of cytochrome *c* in order to enhance precursor formation. In solution, Cr<sup>V</sup> species are often intermediates in Cr<sup>VI</sup> oxidations of organic and biological substrates, e.g. they react rapidly with DNA. There is evidence for implicating Cr<sup>V</sup> species as carcinogens in biosystems featuring interactions of ribonucleotides with added chromate.<sup>[16–19]</sup> The isolation of relatively stable Cr<sup>V</sup> complexes enabled detailed studies into the structures and chemistry of Cr(V).<sup>[20–23]</sup> Cr<sup>IV</sup> has an even more rare oxidation state. In aqueous media alkoxo and porphyrinato complexes of Cr<sup>IV</sup> are generally unstable, while diperoxo triamines [Cr<sup>IV</sup>(O<sub>2</sub>)<sub>2</sub>(NR<sub>3</sub>)<sub>3</sub>] are stable in water for several hours in acidic media.<sup>[24–26]</sup> To stabilize the complex used in this study in aqueous solution, the ligand 2-ethyl-2-hydroxybutyric acid was used in excess.<sup>[27]</sup> The overall redox reaction is given in Scheme 1.



Scheme 1. Reaction between *trans*-bis(2-ethyl-2-hydroxybutanoato(2-))oxochromate(V) and horse heart cytochrome *c*<sup>II</sup>

Higher-valent metallo-oxoporphyrins of iron, manganese and chromium are essential for understanding the mechanisms of enzymatic pathways, e.g. dealing with the oxidation of metalloporphyrins by hydroperoxides in aqueous solution, and with the alkene epoxidation by higher-valent metallo-oxoporphyrins.<sup>[28]</sup> The driving force for studying metalloporphyrin-catalyzed reactions is to develop syn-

thetic species which are able to reproduce and mimic the different heme enzyme-mediated reactions like oxygenation, oxidation, oxidative chlorination, and dismutation.<sup>[29]</sup> The result of ligand-exchange chemistry in water<sup>[30][31]</sup> and with quinic acid in methanol<sup>[32]</sup> showed that 2-hydroxy acids are preferred strongly to 1,2-diols for binding to Cr<sup>V</sup>. Since 2-hydroxy acids, such as citrate and lactate, are present in cells, they may bind to the Cr<sup>V</sup> that is produced intracellularly by reduction of carcinogenic Cr<sup>VI</sup>. They even may show preference for binding to Cr<sup>V</sup>, with respect to 1,2-diol ligands, such as ascorbate, sugars and their derivatives. The biologically relevant analogues to *trans*-bis(2-ethyl-2-hydroxybutanoato(2-))oxochromate(V) are likely to be one type of the Cr<sup>V</sup> species present in the cells that are transformed genetically by exposure to Cr<sup>VI</sup>. This justifies the need to study the reactions of well-characterized model 2-hydroxy acid complexes with DNA.<sup>[18][20]</sup>

Indeed the outer-sphere interaction of the redox partners turned out to be significant and could be accounted for theoretically. In addition, the volume profile constructed for the electron-transfer process clearly reveals a nonsymmetrical nature with respect to the location of the transition state, from which it can be concluded that the process is characterized by a "late" (product-like) transition state. This can be accounted for in terms of the effective precursor complex-formation found for the present system, as compared to the absence of such precursor formation in the case of the ruthenium and cobalt complexes studied before.<sup>[12–14]</sup>

## Results

### Kinetic Studies

The redox reaction was studied under pseudo-first order conditions. The cytochrome concentration was throughout 0.025 mM and the chromium complex in at least a 10-fold

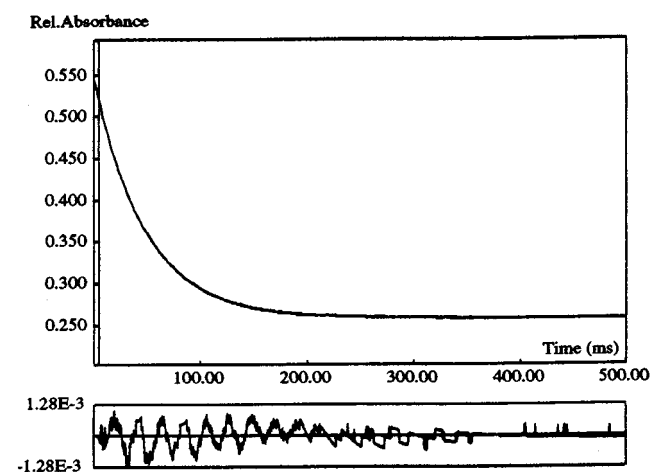


Figure 1. Typical absorbance-time trace fitted with one-exponential decay ( $k_{\text{obs}} = 20.9 \pm 0.009 \text{ s}^{-1}$ ) for  $[\text{Cr}^{\text{V}}] = 0.30 \text{ mM}$ ,  $\text{pH} = 4.8$ ,  $[\text{L}] = 0.0054 \text{ M}$ ,  $T = 15^\circ\text{C}$ ,  $\lambda = 550 \text{ nm}$

excess. A typical absorbance-time trace is shown in Figure 1.

Aqueous acetate buffer solutions in the pH range 3.9 to 5.2 were used for the pH-dependence study reported in

Table 1. Between pH 4.6 and 5.0 the rate remains constant, whereas at pH 4.3 the reaction is accelerated by a factor of 1.5. The concentration dependence (Figure 2) was investigated at pH 4.8, and up to a 400-fold excess of  $\text{Cr}^{\text{V}}$  was used. In order to guarantee the stability of the chromium complex an excess of free ligand was added to the reaction medium. The free ligand concentration was increased even more in another experiment (Figure 2) to check whether there might be some aquation of the chromium complex accompanied by direct binding to cytochrome. These measured points did not differ at all from the former experiments and therefore an inner-sphere mechanism can be excluded.

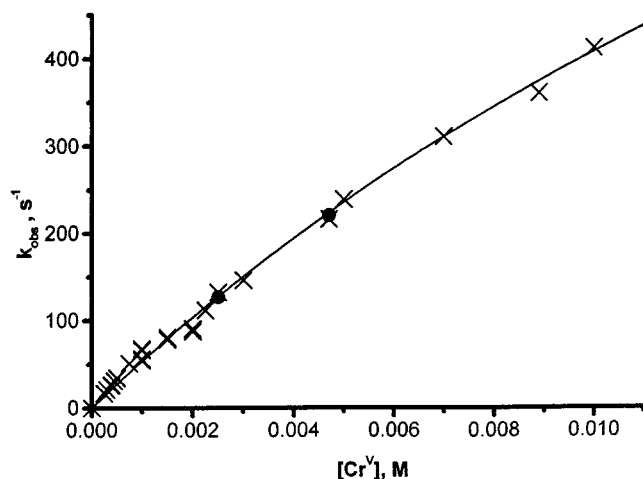


Figure 2. Observed pseudo-first-order rate constant as a function of chromium complex concentration; (x) measured data, except for the one-fold weighted point (0; 0); conditions: pH 4.8;  $[\text{HAc}] = 0.12 \text{ M}$ ,  $[\text{KAc}] = 0.20 \text{ M}$ ,  $[\text{L}] = 0.0054 \text{ M}$ ,  $[\text{LiNO}_3]_{\text{max}} = 0.40 \text{ M}$ ,  $I = 0.6 \text{ M}$ ;  $15^\circ\text{C}$ ; curve results from the best fit based on the kinetic saturation model, Equation 4; influence of increased free ligand concentration on the rate constant was checked (•) (personal suggestion by P. A. Lay to ensure an outer sphere mechanism and to exclude possible direct binding of the chromium complex to cytochrome); conditions: pH 4.8;  $[\text{HAc}] = 0.12 \text{ M}$ ,  $[\text{KAc}] = 0.20 \text{ M}$ ,  $[\text{L}] = 0.10 \text{ M}$ ,  $[\text{LiNO}_3]_{\text{max}} = 0.30 \text{ M}$ ,  $I = 0.6 \text{ M}$ ;  $15^\circ\text{C}$

The observed rate constants clearly show a trend toward saturation at higher  $\text{Cr}^{\text{V}}$  concentrations. A nonlinear least-square fit of the data according to Equation (4) resulted in  $K = 37 \pm 5 \text{ M}^{-1}$  and  $k_{\text{ET}} = 1510 \pm 170 \text{ s}^{-1}$  at  $288 \text{ K}$ . The temperature dependence of the reaction was studied at very low  $\text{Cr}^{\text{V}}$  concentration, i.e. where a linear correlation between  $k_{\text{obs}}$  and  $\text{Cr}^{\text{V}}$  concentration exists. The Eyring plot for the second-order rate constants is given in Figure 3, and the calculated activation parameters are  $\Delta H^\ddagger = 20.9 \pm 0.1 \text{ kJ mol}^{-1}$  and  $\Delta S^\ddagger = -79.9 \pm 0.2 \text{ J K}^{-1} \text{ mol}^{-1}$ . All ambient pressure measurements were performed in acetate buffer mostly at pH 4.8.

Measurements at elevated pressure (up to  $150 \text{ MPa}$ ) were performed at two pH values, above and below pH 4.8, in order to check the possible influence of a shift to lower pH values at higher pressure caused by an increase in the dissociation constant of acetic acid with increasing pressure.<sup>[45]</sup> As a result the pH is not constant during a pressure run. The plots of  $\ln k_{\text{obs}}$  versus pressure are shown in Figure 4, from which it follows that  $\Delta V^\ddagger = -9.2 \pm 0.6$  and  $-11.1$

$\pm 0.8 \text{ cm}^3 \text{ mol}^{-1}$  at  $279 \text{ K}$  and pH 5.0 and 4.7, respectively. The more negative number at the lower pH is consistent with our observation mentioned above that the reaction is accelerated in more acidic solutions, as a result of the increased acid strength of the buffer at elevated pressures.

Cytochrome  $c^{\text{II/III}}$  exhibits a much smaller pressure dependence, and a reaction volume of  $+5 \text{ cm}^3 \text{ mol}^{-1}$  was estimated.<sup>[15]</sup> Therefore, the observed volume of activation mainly results from volume changes on the chromium complex when it changes its overall charge from  $-1$  to  $-2$  during the reduction by cytochrome  $c^{\text{II}}$ . This is also demonstrated by the significantly negative activation entropy, which is in line with a significant increase in electrostriction during the electron-transfer process.

## Electrochemical Studies

In order to construct a volume profile for an irreversible reaction, the activation volume for the reaction and the overall reaction volume, i.e. the difference between the par-

Table 1. Kinetic data for the electron-transfer reaction between  $\text{O}=\text{CrL}_2^{1-}$  and horse-heart cytochrome  $c^{\text{II}}$

$T [^\circ\text{C}]$	pH	$p [\text{MPa}]$	$c(\text{Cr}^{\text{V}}) [\text{mM}]$	$k_{\text{obs}} [\text{s}^{-1}]$	$k_{\text{f}} [\text{M}^{-1} \text{s}^{-1}]$
25.0	5.2	0.1	0.25	$\text{O}=\text{CrL}_2^{1-}$ decomposes	
				$21.28 \pm 0.08$	85100
				$22.43 \pm 0.05$	89700
				$21.40 \pm 0.09$	85600
				$31.4 \pm 0.2$	125500
	4.8	0.1	0.25	cytochrome $c^{\text{II}}$ oxidizes	
				$17.21 \pm 0.05$	68800
				$16.54 \pm 0.12$	66200
				$21.38 \pm 0.07$	71300
				$21.33 \pm 0.05$	71100
15.0	4.8	0.1	0.30	$26.32 \pm 0.05$	69300
				$26.69 \pm 0.05$	66700
				$26.19 \pm 0.09$	65500
				$31.2 \pm 0.2$	69300
				$34.20 \pm 0.09$	68400
			0.40	$34.52 \pm 0.08$	69000
				$35.90 \pm 0.08$	70200
				$51.5 \pm 0.1$	68700
				$54.69 \pm 0.09$	54700
				$56.3 \pm 0.1$	54700
	4.7	0.1	0.75	$68.02 \pm 0.12$	68000
				$66.6 \pm 0.2$	66600
				$66.5 \pm 0.2$	66500
				$81.0 \pm 0.2$	54000
				$78.7 \pm 0.2$	52500
			2.00	$90.1 \pm 0.2$	45000
				$87.9 \pm 0.2$	44000
				$90.9 \pm 0.3$	45500
				$88.9 \pm 0.2$	44000
				$112.3 \pm 0.4$	49900
5.0	4.8	0.1	2.25	$133.0 \pm 0.1$	53200
				$127.2 \pm 0.2$	50800
				$146.6 \pm 0.3$	48900
				$216.3 \pm 1.0$	46000
				$220.6 \pm 1.0$	46900
			4.70*	$238.7 \pm 1.0$	47700
				$310.9 \pm 1.3$	44400
				$360.7 \pm 1.0$	40500
				$411.8 \pm 2.5$	41200
				$11.05 \pm 0.03$	44200
15.0				$16.54 \pm 0.12$	66100
25.0				$22.36 \pm 0.08$	89400
35.0				$29.87 \pm 0.09$	119500

Table 2. Kinetic data for the electron-transfer-reaction between  $\text{O}=\text{CrL}_2^{1-}$  and horse heart cytochrome  $c^{\text{II}}$  (continued)

T [°C]	pH	p [MPa]	C(Cr <sup>V</sup> ) [mM]	$k_{\text{obs}}$ [s <sup>-1</sup> ]	$k_{\text{f}}$ [M <sup>-1</sup> s <sup>-1</sup> ]
5.0	4.8	0.1	0.40	18.3 ± 0.1	45700
15.0				26.2 ± 0.1	65500
25.0				36.1 ± 0.3	90300
35.0				49.3 ± 0.2	123300
5.5				12.3 ± 0.03	
	5.0	6.5	0.25	13.6 ± 0.2	
		25		14.1 ± 0.2	
		35		15.4 ± 0.3	
		60		16.6 ± 0.3	
		95		20.0 ± 0.1	
	4.7	125	0.25	12.9 ± 0.3	
5.5		21		14.1 ± 0.2	
		57		17.5 ± 0.1	
		80		19.2 ± 0.3	
		105		21.1 ± 0.4	
		130		23.9 ± 0.5	
		150			

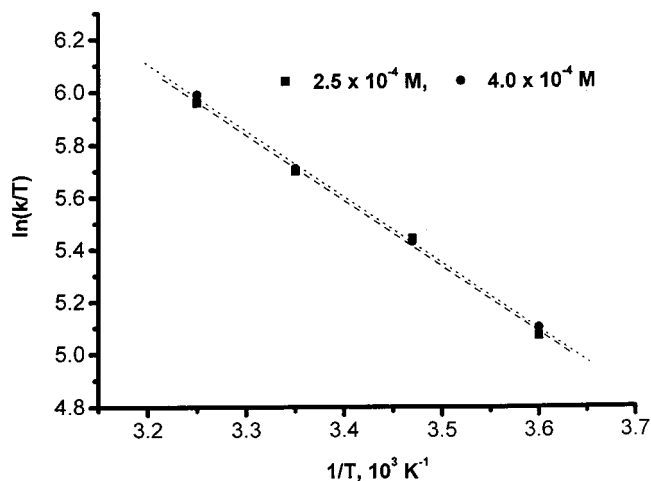
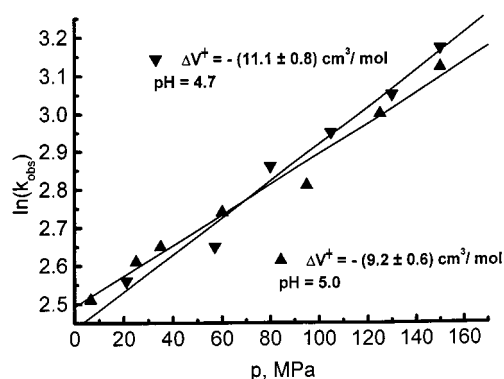
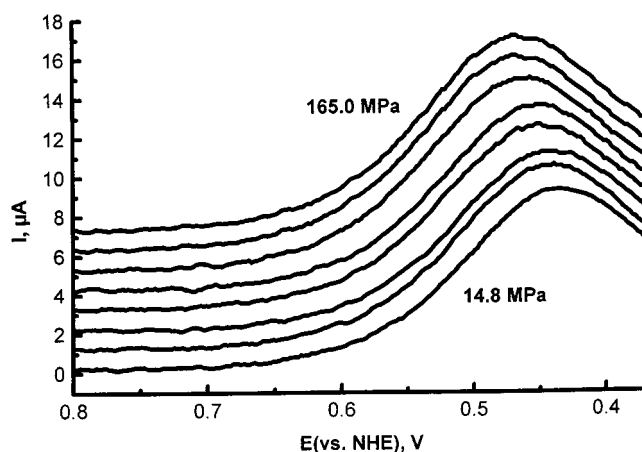
Experimental conditions: [cyt  $c^{\text{II}}$ ] =  $2.5 \cdot 10^{-5}$  M;  $\lambda$  = 550 nm. – pH = 5.2; [HAc] = 0.04 M, [KAc] = 0.20 M, [L] = 0.005 M, [LiNO<sub>3</sub>] = 0.40 M,  $I$  = 0.6 M; pH = 5.0; [HAc] = 0.08 M, [KAc] = 0.27 M, [L] = 0.0082 M, [LiNO<sub>3</sub>]<sub>max</sub> = 0.32 M,  $I$  = 0.6 M; pH = 4.8; [HAc] = 0.12 M, [KAc] = 0.20 M, [L] = 0.0054 M, [LiNO<sub>3</sub>]<sub>max</sub> = 0.40 M,  $I$  = 0.6 M; pH = 4.8; [HAc] = 0.12 M, [KAc] = 0.20 M, [L] = 0.10 M, [LiNO<sub>3</sub>]<sub>max</sub> = 0.30 M,  $I$  = 0.6 M; pH = 4.7; [HAc] = 0.20 M, [KAc] = 0.30 M, [L] = 0.017 M, [LiNO<sub>3</sub>]<sub>max</sub> = 0.31 M,  $I$  = 0.6 M; pH = 4.6; [HAc] = 0.20 M, [KAc] = 0.27 M, [L] = 0.017 M, [LiNO<sub>3</sub>] = 0.31 M,  $I$  = 0.6 M; pH = 4.3; [HAc] = 0.40 M, [KAc] = 0.20 M, [L] = 0.012 M, [LiNO<sub>3</sub>] = 0.39 M,  $I$  = 0.6 M; pH = 3.9; [HAc] = 0.40 M, [KAc] = 0.08 M, [L] = 0.011 M, [LiNO<sub>3</sub>] = 0.51 M,  $I$  = 0.6 M; Calculated activation parameters for  $k_{\text{f}}$ :  $\Delta H^{\ddagger}$  =  $20.9 \pm 0.6$  kJ mol<sup>-1</sup>;  $\Delta S^{\ddagger}$  =  $-79.9 \pm 2.1$  J K<sup>-1</sup> mol<sup>-1</sup>;  $\Delta G^{\ddagger}$  (279 K) =  $43.2$  kJ mol<sup>-1</sup>;  $\Delta V^{\ddagger}$  (pH 5.0 and 279 K) =  $-9.2 \pm 0.6$  cm<sup>3</sup> mol<sup>-1</sup>;  $\Delta V^{\ddagger}$  (pH 4.7 and 279 K) =  $-11.1 \pm 0.8$  cm<sup>3</sup> mol<sup>-1</sup>; intercept  $-(0.1 \pm 0.9)$  s<sup>-1</sup>, resulting from linear fit in the low-concentration range (0.25–0.50 mM Cr<sup>V</sup>); slope  $(55350 \pm 2290)$  M<sup>-1</sup> s<sup>-1</sup>.

Table 3. High-pressure electrochemistry

pH	p [MPa]	$E$ (vs. NHE) [mV]
5.0	0.1	430 ± 1
	22.0	438 ± 1
	49.8	444 ± 1
	75.2	450 ± 1
	95.7	454 ± 1
4.7	125.0	462 ± 1
	14.8	435 ± 1
	24.5	439 ± 1
	49.2	445 ± 1
	73.5	449 ± 1
	95.0	461 ± 1
	123.0	465 ± 1
	146.0	471 ± 1
	165.0	477 ± 1

[Cr<sup>V</sup>] = 5.0 mM, T = 5.5°C, reference electrode (Ag/ 0.01 M AgNO<sub>3</sub>, 1.0 M KNO<sub>3</sub>), scan rate 2 mV s<sup>-1</sup>,  $\Delta V_{\text{corr.}}(\text{Ag}/\text{Ag}^+) = -11.9 \pm 0.5$  cm<sup>3</sup> mol<sup>-1</sup> (25°C,  $I$  = 1.0 M KNO<sub>3</sub>).<sup>[52]</sup>

tial molar volumes of reactant and product species, are required. For the cytochrome  $c^{\text{II/III}}$  system the partial molar volume difference has already been studied.<sup>[15]</sup> The difference in partial molar volume for the Cr<sup>V/IV</sup> system was investigated electrochemically under the same reaction conditions as those selected for the high-pressure stopped-flow experiments. For the electrochemical measurements at

Figure 3. Temperature dependence for 0.25 and 0.40 mM Cr<sup>V</sup> complex concentrations at pH 4.8; [HAc] = 0.12 M, [KAc] = 0.20 M, [L] = 0.0054 M, [LiNO<sub>3</sub>] = 0.40 M,  $I$  = 0.6 MFigure 4. Plot of  $\ln k_{\text{obs}}$  versus pressure. – Conditions: [Cr<sup>V</sup>] = 0.25 mM, 279 K; pH = 5.0; [HAc] = 0.08 M, [KAc] = 0.27 M, [L] = 0.0082 M, [LiNO<sub>3</sub>]<sub>max</sub> = 0.32 M,  $I$  = 0.6 M; pH = 4.7; [HAc] = 0.20 M, [KAc] = 0.30 M, [L] = 0.017 M, [LiNO<sub>3</sub>]<sub>max</sub> = 0.31 M,  $I$  = 0.6 MFigure 5. Differential pulse voltammograms of the Cr<sup>V/IV</sup> couple at pH 4.7 as a function of pressure, recorded at 14.8, 24.5, 49.2, 73.5, 95.0, 146.0 and 165.0 MPa; the traces are offset by arbitrary amounts on the current scale to improve legibility

pressures up to 165 MPa, experiments with CV and DPV were performed. Both techniques are in general comp-

lementary, but DPV showed more reproducible data in the present case.<sup>[46,47,48]</sup> Figure 5 reports the recorded DPVs as a function of pressure.

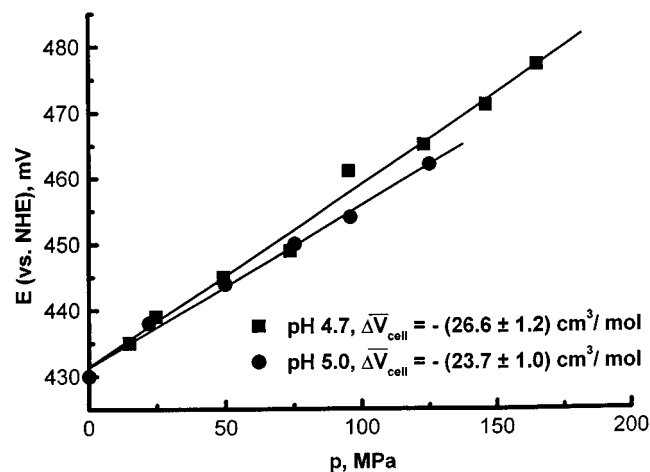


Figure 6. Plot of the redox potential for the  $\text{Cr}^{\text{V/IV}}$  system at pH 5.0 and 4.7 as a function of pressure

The change in redox potential with increasing pressure is moderate, as expected for an overall charge increase from  $-1$  to  $-2$ . The volume change associated with the overall cell reaction was estimated from the plot of the measured redox potential as a function of pressure (Figure 6). The measured  $E_{1/2}$  value for the redox couple at ambient pressure is in good agreement with data reported by other authors.<sup>[49–51]</sup> The reaction volume associated with the  $\text{Cr}^{\text{V/IV}}$  redox couple can now be calculated from the cell reaction volume by subtracting the volume contribution of the reference electrode  $\text{Ag}/\text{AgNO}_3$  which was shown to be  $-11.9 \pm 0.5 \text{ cm}^3 \text{ mol}^{-1}$ .<sup>[52]</sup> The resulting reaction volumes are  $-11.8 \pm 0.5$  (pH 5.0) and  $-14.7 \pm 0.7 \text{ cm}^3 \text{ mol}^{-1}$  (pH 4.7), and reflect the overall volume changes arising from the reduction of  $\text{Cr}^{\text{V}}$  to  $\text{Cr}^{\text{IV}}$ , as well as that caused by a change in the overall charge from  $-1$  to  $-2$ . The solvational effects in terms of a significant increase in electrostriction obviously overrule the intrinsic volume changes in order to account for the overall negative reaction volumes.

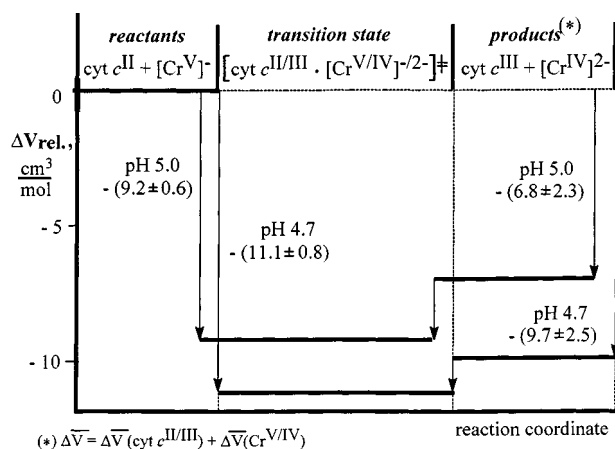


Figure 7. Volume profile for the irreversible reaction of cytochrome  $c^{\text{II}}$  with *trans*-bis(2-ethyl-2-hydroxybutanoato(2-))oxochromate(V)

The employed complex  $[\text{O}=\text{Cr}^{\text{V}}(\text{Lig})_2]^-$  was crystallographically characterized as a five-coordinate oxo compound with a distorted trigonal-bipyramidal geometry.<sup>[53]</sup> At pH 2.5 to 4.0 in the presence of ligand and buffer,  $\text{Cr}^{\text{IV}}$  solutions suffer perceptible loss within a few minutes due to disproportionation,  $2\text{Cr}^{\text{IV}} \rightarrow \text{Cr}^{\text{III}} + \text{Cr}^{\text{V}}$ , and reduction by the parent ligand,  $2\text{Cr}^{\text{IV}} \text{Et}_2\text{C}(\text{OH})\text{COO}^- \rightarrow 2\text{Cr}^{\text{III}} + \text{Et}_2\text{C}=\text{O} + \text{CO}_2 + \text{H}^+$ .<sup>[25][38]</sup> Electrochemical studies have shown that major structural rearrangement follows the electron-transfer process in the  $\text{Cr}^{\text{IV}}/\text{Cr}^{\text{III}}$  system, but not in the  $\text{Cr}^{\text{V}}/\text{Cr}^{\text{IV}}$  couple.<sup>[51]</sup> The suggestion that a third ligand will enter the coordination sphere at the vacant site on  $\text{Cr}^{\text{V}}$  was disregarded later on.<sup>[35]</sup> The formation of six-coordinate forms is much less likely for complexes with the more bulky ligands. The  $\text{Cr}^{\text{V}}$  complex has a distorted trigonal-bipyramidal geometry, whereas the  $\text{Cr}^{\text{IV}}$  complexes are likely to remain as five-coordinate oxo complexes, like their  $\text{Cr}^{\text{V}}/\text{Cr}^{\text{V}}$  analogues. There is no evidence for  $\text{Cr}^{\text{V}}$  complexes containing three chelate ligands and such complexes are not expected to form for steric reasons. The redox potential for  $\text{Cr}^{\text{IV/III}}$  is more positive, which means that it is a stronger oxidizing agent than  $\text{Cr}^{\text{V/IV}}$ . The quasi-reversible one-electron redox process (corresponding to  $\text{Cr}^{\text{V}} + e^- \rightleftharpoons \text{Cr}^{\text{IV}}$ ) can only be observed at the electrode surface because there is a lack of conversion of  $\text{Cr}^{\text{IV}}$  to  $\text{Cr}^{\text{III}}$  due to an extremely slow electrokinetic process for the reduction of the  $\text{Cr}^{\text{IV}}$  intermediates.<sup>[24]</sup>  $\text{Cr}^{\text{IV}}$  exists mainly in the form of bis-chelated complexes. The stability of  $\text{Cr}^{\text{IV}}$  complexes exhibits a bell-shaped pH dependence. The region of maximum stability and the corresponding half-life ( $[\text{Cr}^{\text{IV}}]_0 = 0.1 \text{ mM}$ ;  $25^\circ\text{C}$ ) is 30 min at  $\text{pH} \approx 3$ . Half-lives were determined from the absorbance changes at 550 nm, where the absorbances of  $\text{Cr}^{\text{III}}$  and  $\text{Cr}^{\text{V}}$  complexes were negligible in comparison with that of  $\text{Cr}^{\text{IV}}$ .<sup>[25]</sup> The important difference in the chemical properties of  $\text{Cr}^{\text{IV}}$  and  $\text{Cr}^{\text{V}}$  is that 2-hydroxy carboxylates are much poorer ligands for  $\text{Cr}^{\text{IV}}$  than for  $\text{Cr}^{\text{V}}$ . This is probably the result of the lower acidity of the ROH groups bound to  $\text{Cr}^{\text{IV}}$ . Thus, the ROH groups remain largely protonated at pH 2 to 4, whereas those of the corresponding  $\text{Cr}^{\text{V}}$  complexes are fully deprotonated under these conditions.<sup>[25]</sup>

## Saturation Kinetics

In order to account for the experimentally observed rate constants as a function of the  $\text{Cr}^{\text{V}}$  concentration, the Fuoss theory was applied.<sup>[10]</sup> The reaction conditions are water as solvent at 279 K and 0.6 M ionic strength. Even at high ionic strength, the acetate shows no specific binding ability for cytochrome.<sup>[74]</sup> This should be the same for the ligand, which is added in excess in order to stabilize the complex and is very similar in structure. In addition, the number of protein-bound nitrates, two in the reduced and one in the oxidized form, is independent of the anion concentration.<sup>[74]</sup> The adopted permittivity leads to a reciprocal Debye-Hückel radius of 2.52 nm.<sup>[54]</sup> There are three possible positions for negative charges on the  $\text{Cr}^{\text{V}}$  complex,

viz. the oxo group, the ring carboxylate oxygen, and the carboxylate oxygen, which are all exposed to solvent water. The ring hydroxo group is sterically hindered by the bulky ethyl groups. For the evaluation of the contact radius for the chromium complex, the X-ray structure and different van der Waals radii for oxygen are available.<sup>[55,56–58]</sup> The contact radius for cytochrome *c* was estimated to be 1.66 nm.<sup>[59]</sup> A combination of these values result in a contact distance in the range between 1.82 and 2.21 nm. The outer-sphere preequilibrium constant *K* and the associated rate constant *k*<sub>ET</sub> were now calculated by varying the possible ionic charge on the cytochrome center. Since the chromium reactant carries an overall charge of  $-1$ , and the enzyme has a net charge of  $+6.5$ ,<sup>[59]</sup> the product of the ionic charges can adapt theoretical values between  $-1$  and  $-6.5$ , depending on to what extent charge is neutralized by the presence of counter ions and local charge effects influence the electron-transfer process. Both *K* and *k*<sub>ET</sub> increase more on increasing the contact radius of the chromium complex than on changing the effective ionic charge. On the basis of a 75% agreement between the values calculated with the Fuoss Equation and those obtained in the kinetic measurements, the product of the ionic charges should be at least 1.5 for Cr...C=O, 6.5 for Cr–O and 7.0 for Cr=O. However, the following aspects should also be considered: electrostatic interactions in the precursor complex are assigned to a larger extent to charge localized at the haem crevice than to the sum of all charges;<sup>[60][61]</sup> lysine 13, 72, 86 and Histidin 33 (at pH values below its *pK*<sub>a</sub> of 6.4) show kinetic relevance for anionic redox partners and a local charge of  $+3$  to  $+4$  on the cytochrome surface was estimated from kinetic measurements as a function of ionic strength.<sup>[62–66]</sup> Based on this information, conclusions can be reached with respect to the three possible contact radii. The most probable position for charge localization on the chromium complex is the Cr...C=O group, which is more likely than the Cr–O group and in turn much better than the Cr=O position. This is in agreement with some classical explanations.<sup>[67]</sup> In summary, the results from the kinetic studies are consistent with predictions on the basis of the Fuoss postulations.

The thermal and pressure activation parameters were determined at low Cr<sup>V</sup> concentrations due to the time resolution of the kinetic equipment, with the result that the observed second-order rate constant is a composite function and represents *K*·*k*<sub>ET</sub>. The observed entropy and volume of activation are both significantly negative and indicate a highly-structured transition state. More mechanistic insight can be gained from an analysis of the volume profile for the overall process.

### Volume Profile

The molar volume change associated with the redox couple cytochrome *c*<sup>II/III</sup> was estimated to be  $+(5.0 \pm 0.8) \text{ cm}^3 \text{ mol}^{-1}$ .<sup>[15]</sup> This value indicates that there is a slight increase in the partial molar volume of cytochrome *c*<sup>II</sup> during the

oxidation process, even though the overall charge increases from  $+6.5$  to  $+7.5$ , which is expected to cause a solvational volume collapse due to an increase in electrostriction. A number of reports in the literature report a more compact structure for the reduced protein as compared to cytochrome *c*<sup>III</sup>.<sup>[59,68–71]</sup> However, the increase in the size of the protein results in the partial accommodation of water molecules from the bulk in the protein framework. A small overall volume increase is therefore obtained.<sup>[65]</sup> It is assumed that the volume change on cytochrome *c* is the same at pH 5 and 7. Cytochrome does not show any pH dependence in this pH range; deviations only occur at  $\text{pH} \geq 8.0$ .<sup>[6,12,73]</sup> In order to calculate the overall reaction volume, the contribution arising from the Cr<sup>V/IV</sup> complex has to be added (see Figure 7). We found that a significant volume collapse accompanies this reduction process (see electrochemical studies).

Detailed electrochemical measurements as a function of pressure resulted in a good correlation between the volume changes associated with changes in electrostriction and the change in the overall charge on the complex.<sup>[52]</sup> As a useful working rule the electrostrictive volume changes by ca.  $4 \text{ cm}^3 \text{ mol}^{-1}$  per unit difference in the square of the charge on the oxidized and reduced forms of the complex. In the present case this difference is 3, from which an electrostrictive volume collapse of ca.  $12 \text{ cm}^3 \text{ mol}^{-1}$  can be predicted. By way of comparison, the experimental values reported for the couples  $\text{Fe}(\text{phen})(\text{CN})_4^{1-/2-}$  and  $\text{Fe}(\text{bpy})(\text{CN})_4^{1-/2-}$  are  $-13.6$  and  $-13.8 \text{ cm}^3 \text{ mol}^{-1}$ , respectively.<sup>[52]</sup> From this it follows that the solvational volume changes due to a significant increase in electrostriction, represent the major contribution toward the overall negative reaction volumes found in this study. The oxidation of cytochrome *c*<sup>II</sup> by the Cr<sup>V</sup> oxo species is therefore associated with a moderate overall volume decrease of  $-7$  and  $-10 \text{ cm}^3 \text{ mol}^{-1}$  (see Figure 7). The location of the transition state can be described as "late" in terms of the overall volume change and is close to the product state. This can at present only be related to the efficient precursor formation occurring in the system.

In contrast, the investigated Co<sup>III/II</sup> and Ru<sup>III/II</sup> systems referred to in the Introduction show no kinetic evidence for precursor formation and exhibit very similar volume changes for both the forward and reverse electron-transfer reactions.<sup>[12–14]</sup> The ruthenium complexes exhibit negligible intrinsic volume changes and therefore mainly solvational effects account for the observed volume changes.<sup>[12]</sup> In the case of the Co<sup>III/II</sup> systems, there is a volume increase due to a decrease in solvent electrostriction and an intrinsic contribution.<sup>[14]</sup> Both these systems involve large volume changes, and the transition state lies almost exactly halfway between the partial molar volumes of the reactants and products in the reported volume profiles. This means that the reorganisation in the transition state is very similar for both the forward and back reactions in the reversible electron-transfer process in the absence of significant precursor formation. The nonsymmetrical nature of the volume profile found in the present study must therefore be related to

the effective formation of a precursor species. A similar situation was recently encountered in the volume profiles for a series of intramolecular electron-transfer reactions of ruthenated cytochrome *c* systems.<sup>[72]</sup> In that case different possible explanations for the nonsymmetric appearance of the volume profiles were presented. It is our objective in future work to search for redox systems involving cytochrome *c* that will exhibit an even more efficient precursor formation in order to be able to determine a volume profile for the electron-transfer reaction within the precursor species, i.e. under conditions of saturation kinetics where electron transfer is the rate determining step, something that was not possible in the present study.

## Conclusions

The outer-sphere electron-transfer reaction between horse-heart cytochrome *c* and anionic trans-bis(2-ethyl-2-hydroxybutanoato(2-))oxochromate showed a clear trend towards rate saturation, which is rather unusual for cytochrome and its interaction with small reaction partners. The precursor formation constant and the electron-transfer rate constant could be separated kinetically. In order to account for the experimentally observed rate constants as a function of the Cr<sup>V</sup> concentration, the Fuoss theory was applied. It revealed additional information that the contact between both reactants occurs most probable with the solvent exposed carboxylate oxygen on chromium. Measured activation and reaction volumes at two pH values enabled the construction of a volume profile for the reaction which differs significantly from the symmetric volume profiles reported for outer-sphere electron-transfer reactions of cobalt and ruthenium complexes. Information regarding the location of the reaction coordinate could be obtained.

## Experimental Section

**Methods:** UV/vis spectra were recorded on either a Hewlett–Packard HP8452 or a Shimadzu UV-2101PC spectrophotometer. – IR spectra were measured in KBr disks on a Mattson Polaris 10410R FT-IR spectrometer. – A Bruker ESP 300E X-band spectrometer operating at about 9.5 GHz was used for recording EPR spectra of solutions contained in a quartz flat cell. EPR spectrometer settings were as follows: central field, 3480 G; sweep width, 100 G; microwave power, 10.1 mW; modulation frequency, 100 kHz; modulation amplitude, 0.974 G; receiver gain,  $1.25 \times 10^3$ ; conversion time, 20.48 ms; time constant, 10.24 ms; number of scans, 1; temperature 298 K. – The pH of the solutions was measured on a Metrohm 716 DMS Titrino pH-meter. The kinetic traces for the reduction of cytochrome *c* were recorded at 550 nm. The reactions at ambient pressure were followed using an Applied Photophysics SX-18 MV stopped-flow instruments (Leatherhead, UK), to which an online data acquisition system was connected. The kinetic traces, consisting of 1000 points per trace, were collected, stored and fitted on an Acorn 5000 computer using Applied Photophysics software (Leatherhead, UK). In order to observe the progress of the overall reaction, time resolved spectra were recorded on an Applied Photophysics SX-18 MV stopped-flow instrument (Leatherhead, UK) equipped with a J&M TIDAS 16–500 diode array detector (Aalen,

Germany). A homemade high-pressure stopped-flow system was used for the high pressure kinetic measurements.<sup>[39][40]</sup> The kinetic traces consisting of 1000 points per trace, were collected and stored on an IBM-compatible computer using Biologic (Claix, France) software. The rate constants were calculated using the OLIS KINFIT program (Olis, Bogart, Georgia, USA). All Instruments were thermostated to  $\pm 0.1^\circ\text{C}$ . The kinetic traces showed excellent first-order behavior over 5 half-lives. – In general, all solutions were prepared under nitrogen to avoid complications with dissolved oxygen. All test solutions were protected from light to avoid photoinduced decomposition.<sup>[41]</sup> The freshly prepared solutions were transferred into the stopped-flow unit using gastight Optima Graf Fortuna glass syringes (Roth). All experiments were performed in acetate buffer of different pH values. – Electrochemical measurements were performed with an EG&G Princeton Applied Research 263 System; the data were stored and fitted using Model 270/250 Research Electrochemistry Software 4.00. For electrochemical measurements at elevated pressure, a homemade, high-pressure cell similar to that described in the literature<sup>[42]</sup> and thermostated to  $\pm 0.1^\circ\text{C}$ , was employed. Prior to use, the glassy carbon electrode surface was polished with an aqueous suspension of 3 micron followed by 1 micron alumina (Alfa) on a polishing cloth, followed by rinsing with distilled water and further cleaning with a dry tissue. The Pt plate auxiliary electrode was cleaned in 5 M aqueous HNO<sub>3</sub>, rinsed with distilled water and dried with a tissue. The reference electrode consisted of a Ag wire in 0.01 M AgNO<sub>3</sub> and 1.0 M KNO<sub>3</sub> solution. The chromium solutions were filled into the electrochemical cell under nitrogen. Nitrogen was passed through the solution for another few minutes to assure that oxygen is absent. The potassium hexacyanoferrate couple was used as external standard. All Differential Pulse Voltammetric (DPV) measurements were performed under the following conditions: pulse height 25 mV, pulse weight 50 ms, scan rate 2 (pH 5.0) and 4 mV s<sup>-1</sup> (pH 4.7). Voltammograms were scanned in the negative direction. For all analyses and plots, Excel<sup>[43]</sup> and Origin<sup>[44]</sup> software was used except when otherwise stated.

**Caution:** Cr<sup>V</sup> complexes are mutagenic, cleave DNA rapidly *in vitro*, and are potentially carcinogenic.<sup>[18][33]</sup> Contact with skin and inhalation must be avoided.

**Reagents:** Horse-heart cytochrome *c* (type VI, Sigma) was purified and reduced as reported before.<sup>[13]</sup> The concentrations of the cytochrome solutions were determined by UV/vis spectroscopy. Sodium bis(2-ethyl-2-hydroxybutanoato(2-))oxochromate(V) was synthesized following the method of Krumpolc and Rocek and was recrystallized from acetone-chloroform.<sup>[34][35]</sup> – Anal. calcd for C<sub>12</sub>H<sub>22</sub>CrNaO<sub>8</sub>: C 39.03; H 6.01; found: C 39.58; H 6.44). – The IR spectra shows  $\tilde{\nu}(\text{Cr}=\text{O})$  (cm<sup>-1</sup>) = 996 (ref. 998, 1000) and  $\tilde{\nu}(\text{C}=\text{O})$  = 1677 (s) (ref. 1660, 1683).<sup>[20,36,37]</sup> In the UV/vis range the complex exhibited a maximum at 510 nm with an extinction coefficient of 165 M<sup>-1</sup> cm<sup>-1</sup> in aqueous solution, which is in agreement with literature data.<sup>[34][35]</sup> The X-band EPR spectra of the sample (ca. 0.002 M) in buffer solution of pH 5.0 shows a single main peak  $g = 1.984$  (<sup>52</sup>Cr,  $I = 0$ ) with four small lines due to the hyperfine coupling with <sup>53</sup>Cr ( $I = 3/2$ , 9.54% natural abundance; hyperfine coupling constant 18.3 Gauss).<sup>[20,35,38]</sup> – The following chemicals were used in the preparation of the reaction solutions: 2-ethyl-2-hydroxybutyric acid (99%), potassium acetate (KAc) and acetic acid (HAc) (Aldrich), and lithium nitrate (Fluka). All commercial reagents were of analytical grade and were used without further purification. Solutions of Cr<sup>V</sup> were prepared by dissolving the synthesized sodium salt of the complex in the buffer solutions under nitrogen directly before use.

## Acknowledgments

The authors are grateful to the Deutsche Forschungsgemeinschaft (Gratuierten Kolleg "Homogener und Heterogener Elektronen-transfer") for support of this project.

- [1] S. Wherland, H. B. Gray, *Biological Aspects of Inorganic Chemistry*, John Wiley, New York, **1977**, p 289.
- [2] G. R. Moore, E. G. S. Eley, G. Williams, *Advances in Inorganic and Bioinorganic Mechanisms* (Ed.: A. G. Sykes), Academic Press, London, **1984**, vol. 3, p 1.
- [3] P. L. Drake, R. T. Hartshorn, J. M. McGinnis, A. G. Sykes, *Inorg. Chem.* **1989**, 28, 1361–1366.
- [4] W. G. Miller, M. A. Cusanovitch, *Biophys. Struct. Mech.* **1975**, 1, 97–111.
- [5] J. Butler, D. M. Davies, A. G. Sykes, *J. Inorg. Biochem.* **1981**, 15, 41–53.
- [6] H. L. Hodges, R. A. Holwerda, H. B. Gray, *J. Am. Chem. Soc.* **1974**, 3132–3137.
- [7] S. Speh, Ph. D. Thesis, Technical University of Darmstadt, Germany, **1993**.
- [8] J. K. Yandell, D. P. Fay, N. Sutin, *J. Am. Chem. Soc.* **1973**, 95, 1131–1137.
- [9] [9a] C. Creutz, N. Sutin, *Proc. Nat. Acad. Sci. U.S.A.* **1973**, 70, 1701–1703. [9b] D. O. Lambeth, G. Palmer, *J. Biol. Chem.* **1973**, 248, 6095–6103.
- [10] R. M. Fuoss, *J. Am. Chem. Soc.* **1958**, 80, 5059–5061.
- [11] R. D. Cannon, *Electron Transfer Reactions*, Butterworth, London, **1980**, chapter 4.2.
- [12] M. Meier, J. Sun, J. F. Wishart, R. van Eldik, *Inorg. Chem.* **1996**, 35, 1564–1570.
- [13] B. Bansch, M. Meier, P. Martinez, R. van Eldik, C. Su, J. Sun, S. S. Isied, *Inorg. Chem.* **1994**, 33, 4744–4749.
- [14] M. Meier, R. van Eldik, *Chem. Eur. J.* **1997**, 3, 39–46.
- [15] J. Sun, J. F. Wishart, R. van Eldik, R. D. Shalders, T. W. Swaddle, *J. Am. Chem. Soc.* **1995**, 117, 2600–2605.
- [16] D. M. Goodgame, P. B. Hayman, D. F. Hathaway, *Polyhedron* **1982**, 1, 497–499.
- [17] S. Kawanishi, S. Inoue, S. Sand, *J. Biol. Chem.* **1986**, 261, 5952–5958.
- [18] R. P. Farrell, R. J. Judd, P. A. Lay, N. E. Dixon, R. S. U. Baker, A. M. Bonin, *Chem. Res. Toxicol.* **1989**, 2, 227–229.
- [19] R. N. Bose, S. Moghaddas, E. Gelerinter, *Inorg. Chem.* **1992**, 31, 1987–1994.
- [20] R. P. Farrell, P. A. Lay, *Comments Inorg. Chem.* **1992**, 13, 133–175.
- [21] R. Colton, *Coord. Chem. Rev.* **1985**, 62, 85–130.
- [22] M. Mitewa, P. R. Bontchev, *Coord. Chem. Rev.* **1985**, 61, 241–272.
- [23] J. K. Beattie, G. P. Haight, Jr., *Prog. Inorg. Chem.* **1972**, 17, 93–145.
- [24] R. N. Bose, B. Fonkeng, G. Barr-David, R. P. Farrell, R. J. Judd, P. A. Lay, D. F. Sangster, *J. Am. Chem. Soc.* **1996**, 118, 7139–7144.
- [25] R. Codd, P. A. Lay, A. Levina, *Inorg. Chem.* **1997**, 36, 5440–5448.
- [26] E. S. Gould, *Coord. Chem. Rev.* **1994**, 135/136, 651–684.
- [27] N. Rajasekar, R. Subramaniam, E. S. Gould, *Inorg. Chem.* **1983**, 22, 971–975.
- [28] R. D. Arasasingham, T. C. Bruice, *The Activation of Dioxygen and Homogeneous Catalytic Oxidation* (Ed.: D. H. R. Barton), Plenum Press, New York, **1993**, p 147–169.
- [29] B. Meunier, *Chem. Rev.* **1992**, 92, 1411–1456.
- [30] R. Bramley, J.-Y. Ji, P. A. Lay, *Inorg. Chem.* **1991**, 30, 1557–1569.
- [31] M. Charara, B. Sc. Thesis, University of Sydney, Australia, **1988**.
- [32] G. Barr-David, M. Charara, R. Codd, R. P. Farrell, J. A. Irwin, P. A. Lay, R. Bramley, S. Brumby, J.-Y. Ji, G. R. Hanson, *J. Chem. Soc., Faraday Trans.* **1995**, 91, 1207–1216.
- [33] C. T. Dillon, P. A. Lay, A. M. Bonin, N. E. Dixon, T. J. Collins, K. L. Kostka, *Carcinogenesis* **1993**, 14, 1875–1880.
- [34] M. Krumpolc, J. Rocek, *J. Am. Chem. Soc.* **1979**, 101, 3206–3209.
- [35] Y.-T. Fanchiang, R. N. Bose, E. Gerinter, E. S. Gould, *Inorg. Chem.* **1985**, 24, 4679–4684.
- [36] R. Bramley, R. P. Farrell, J.-Y. Ji, P. A. Lay, *Aust. J. Chem.* **1990**, 43, 263–279.
- [37] M. Krumpolc, B. G. DeBoer, J. Rocek, *J. Am. Chem. Soc.* **1978**, 100, 145–153.
- [38] M. C. Ghosh, E. Gelerinter, E. S. Gould, *Inorg. Chem.* **1992**, 31, 702–705.
- [39] vanR. Eldik, D. A. Palmer, R. Schmidt, H. Kelm, *Inorg. Chim. Acta* **1981**, 50, 131–135.
- [40] vanR. Eldik, W. Gaede, S. Wieland, J. Kraft, M. Spitzer, D. A. Palmer, *Rev. Sci. Instrum.* **1993**, 64, 1355–1357.
- [41] M. Krumpolc, J. Rocek, *Inorg. Chem.* **1985**, 24, 617–621.
- [42] H. Doine, T. W. Whitcombe, T. W. Swaddle, *Can. J. Chem.* **1992**, 70, 81–88.
- [43] Excel, Version 5.0, Microsoft Software, **1993**.
- [44] Origin. Technical Graphics and Data Analysis for Windows, Version 4.1, Microcal Software, Inc., Northampton, MA, **1996**.
- [45] Y. Kitamura, T. Itoh, *J. Solution Chem.* **1987**, 16, 715–725.
- [46] J. Osteryoung, *J. Chem. Educ.* **1983**, 60, 296.
- [47] G. A. Mabott, *J. Chem. Educ.* **1983**, 60, 697.
- [48] K. K. Rodgers, S. G. Sligar, *J. Am. Chem. Soc.* **1991**, 113, 9419–9421.
- [49] R. N. Bose, V. D. Neff, E. S. Gould, *Inorg. Chem.* **1986**, 25, 165–168.
- [50] J. M. Eckert, R. J. Judd, P. A. Lay, *Inorg. Chem.* **1987**, 26, 2189–2191.
- [51] R. N. Bose, B. Fonkeng, G. Barr-David, R. P. Farrell, R. J. Judd, P. A. Lay, D. F. Sangster, *J. Am. Chem. Soc.* **1996**, 118, 7139–7144.
- [52] J. I. Sachanidis, R. D. Shalders, P. A. Tregloan, *Inorg. Chem.* **1994**, 33, 6180–6186.
- [53] R. J. Judd, T. W. Hambley, P. A. Lay, *J. Chem. Soc., Dalton Trans.* **1989**, 2205–2210.
- [54] H. Landolt, R. Börnstein, A. Eucken, *Zahlenwerte und Fakten aus Physik, Chemie, Astronomie, Geophysik, Technik*, Springer-Verlag, Berlin, **1959**, II. Band, 6. Teil Elektrische Eigenschaften I, p 767.
- [55] For the carboxylate oxygen the Cr...C=O distance was calculated by using the available bond distances and angles, and assuming that the five-membered chelate ring is planar. Distortion at the ring is negligible.
- [56] F. A. Cotton, G. Wilkinson, P. L. Gaus, *Grundlagen der Anorganischen Chemie*, VCH, Weinheim, **1990**, p 97.
- [57] R. A. Marcus, *J. Chem. Phys.* **1957**, 26, 867–871.
- [58] A. Bondi, *J. Phys. Chem.* **1964**, 68, 441–451.
- [59] K. Heremans, M. Bormans, J. Snauwaert, H. Vandersypen, *Faraday Discuss. Chem. Soc.* **1982**, 74, 343–348.
- [60] T. E. Meyer, J. A. Watkins, C. T. Przysiecki, G. Tollin, M. A. Cusanovich, *Biochem.* **1984**, 23, 4761.
- [61] S. K. Chapman, J. D. Sinclair-Day, A. G. Sykes, S. C. Tam, R. J. P. Williams, *J. Chem. Soc. Chem. Commun.* **1983**, 1152–1154.
- [62] J. Butler, S. K. Chapman, D. M. Davies, A. G. Sykes, S. H. Speck, N. Osheroff, E. Margolias, *J. Biol. Chem.*, **1983**, 258, 6400–6404.
- [63] J. Butler, D. M. Davies, A. G. Sykes, W. H. Koppenol, N. Osheroff, E. Margolias, *J. Am. Chem. Soc.* **1981**, 103, 469–471.
- [64] C. G. S. Eley, G. R. Moore, G. Williams, R. J. P. Williams, *Eur. J. Biochem.* **1982**, 124, 295–303.
- [65] R. Margalit, A. Schejter, *Eur. J. Biochem.* **1973**, 32, 492–499.
- [66] T. Goldkorn, A. Schejter, *J. Biol. Chem.* **1979**, 254, 12562.
- [67] The oxo group shifts electron density to the chromium center (weak back bonding from Cr). The ethyl groups increase the electron density on the carboxylate group (inductive effect).
- [68] A. M. Berghuis, G. D. Bryer, *J. Mol. Biol.* **1992**, 223, 959–976.
- [69] Y. Feng, H. Roder, S. W. Englander, *Biochemistry* **1990**, 29, 3494–3504.
- [70] G. Liu, C. A. Grygon, T. G. Spiro, *Biochemistry* **1989**, 28, 5046–5050.
- [71] J. Trehwella, V. A. P. Carlson, E. H. Curtis, D. B. Heidorn, *Biochemistry* **1988**, 27, 1121–1125.
- [72] J. Sun, C. Su, M. Meier, S. S. Isied, J. F. Wishart, R. van Eldik, *Inorg. Chem.*, in press.
- [73] T. Ikeshoji, K. Taniguchi, F. M. Hawkridge, *J. Electroanal. Chem.* **1989**, 270, 297–308.
- [74] G. Battistuzzi, M. Borsari, D. Dallari, I. Lancellotti, M. Sola, *Eur. J. Biochem.* **1996**, 241, 208–214.

Received March 31, 1999

Received March 31, 1999  
[199112]